Early evolution of the ecdysozoan body plan

Deng Wang[1]†, Yaqin Qiang[2]†, Junfeng Guo[2]*, Jean Vannier[3]†, Zuchen Song[2], Jiaxin Peng[2], Boyao Zhang[2], Jie Sun[1,2], Yilun Yu[4,5], Yiheng Zhang[6], Tao Zhang[6], Xiaoguang Yang[1], Jian Han[1]*

[1] State Key Laboratory of Continental Dynamics, Shaanxi Key Laboratory of Early Life & Environments and Department of Geology, Northwest University; Xi'an, China. [2] School of Earth Science and Resources, Key Laboratory of Western China's Mineral Resources and Geological Engineering, Ministry of Education, Chang'an University; Xi'an, China. [3] Université de Lyon, Université Claude Bernard Lyon 1, ENS de Lyon, CNRS, Laboratoire de Géologie de Lyon: Terre, Planètes, Environnement (CNRS-UMR 5276), Villeurbanne 69622, France. [4] University of Chinese Academy of Sciences; Beijing, China. [5] Institute of Vertebrate Paleontology and Paleoanthropology, Chinese Academy of Sciences; Beijing, China. [6] School of Information Science and Technology, Northwest University; Xi'an, China. † These authors contributed equally.
* Correspondence authors: junfengg@chd.edu.cn (J.G); elihanj@nwu.edu.cn (J.H.).

Abstract

Extant ecdysozoans (moulting animals) are represented by a great variety of vermiform or articulated organisms. However, controversies remain about the nature of their ancestral body plan although the vermiform hypothesis seems to prevail. We describe here *Beretella spinosa* gen et sp. nov. a tiny ecdysozoan from the early Cambrian, Yanjiahe Formation, South China, with an unusual sack-like appearance, single opening, and spiny ornament. *Beretella* has no equivalent among animals, except *Saccorhytus* from the basal Cambrian. Phylogenetic analyses resolve both forms as a sister group (Saccorhytida) to all known Ecdysozoa, thus suggesting that ancestral ecdysozoans may have been non-vermiform animals. Saccorhytids are likely to represent an early dead-end off-shot along the stem-line Ecdysozoa that possibly evolved through anatomical simplification (e.g. lack of anus). Although extinct during the Cambrian, this animal lineage provides precious insight into the early evolution of Ecdysozoa and the nature (possibly non-vermiform) of the earliest representatives of the group.

Introduction

The Ediacaran–Cambrian transition is marked by the appearance in the fossil record of a variety of new body plans that prefigure the majority of present-day animal lineages, including the ecdysozoans a huge clade that encompasses all invertebrate animals growing through successive moulting stages, such as panarthropods (Arthropoda, Onychophora, Tardigrada), scalidophoran (incl.

Priapulida) and nematoid worms(Erwin, 2020). Altogether ecdysozoans represent a very high percentage of animal biodiversity and disparity, inhabiting almost all possible ecological niches on Earth(Brusca et al., 2016). The nature of the last common ancestor of Ecdysozoa (LCAE) remains largely unresolved, even though worms are prevalent before the rise of panarthropods as trace and body fossils in basal Cambrian and late Ediacaran rocks(Buatois et al., 2014; Liu et al., 2014; Vannier et al., 2010). Some molecular phylogenies also predict that the most basal ecdysozoans were vermiform organisms(Howard et al., 2022; Laumer et al., 2019) that possibly diverged in the Ediacaran (Howard et al., 2022; Rota-Stabelli et al., 2013). Current reconstruction based on fossil and developmental evidence features the ancestral ecdysozoan as a millimeter-sized worm(Budd, 2001; Valentine and Collins, 2000) with a terminal(Ortega-Hernandez et al., 2019) or ventral mouth (Martín-Durán and Hejnol, 2015; Nielsen, 2019). Clearly, the discovery of *Saccorhytus*(Han et al., 2017; Liu et al., 2022; Shu and Han, 2020b) in the basal Cambrian of China (Kuanchuanpu Formation; ca. 535 Ma(Sawaki et al., 2008)) that is anything but a worm sowed doubt among scientists. *Saccorhytus* is a sac-like secondarily phosphatized microscopic animal spiked with conical sclerites and a single opening that was first seen as the earliest known deuterostome(Han et al., 2017) but is now considered as an ecdysozoan on more solid grounds(Liu et al., 2022; Shu and Han, 2020b), thus broadening the anatomical spectrum of the group and its disparity in the Cambrian and reopening the debate on the nature of LCAE.

We describe here *Beretella spinosa* gen. et sp. nov. from Member 5 of the Yanjiahe Formation (basal Cambrian Stage 2, ca. 529 Ma, Hubei Province, China) that shares morphological traits with *Saccorhytus* such as an ellipsoidal body, a pronounced bilaterality, a spiny ornament made of broad-based sclerites, and a single opening. Cladistic analyses are made to resolve the position of both *Beretella* and *Saccorhytus* that provide key information on the early evolution of the group.

Systematic palaeontology

Superphylum Ecdysozoa Aguinaldo et al.(Aguinaldo et al., 1997)
Phylum Saccorhytida Han, Shu, Ou and Conway Morris, 2017 stat. nov.

Remarks. Saccorhytida first appeared in the literature as a new stem-group Deuterostomia that accommodated a single species, *Saccorhytus coronarius*(Han et al., 2017). Since *Saccorhytus* is no longer considered a primitive deuterostome and, instead, more likely belongs to ecdysozoans, Saccorhytida became an extinct Order of Ecdysozoa(Liu et al., 2022; Shu and Han, 2020b). Because both *Saccorhytus* and *Beretella* display major morphological differences with all other known ecdysozoan phyla (Nematoida, Scalidophora, and Panarthropoda), Saccorhytida is tentatively elevated here

to the rank of phylum within Ecdysozoa.

Emended diagnosis. Microscopic, ellipsoidal body shape with pronounced bilateral symmetry expressed by paired spiny sclerites. Single, presumably oral opening on assumed ventral side (no anus).

Remarks. Only two forms, *Saccorhytus* and *Beretella* are currently placed within Saccorhytida, making it premature to formally define intermediate taxonomic categories such as an order and a family.

Beretella spinosa Han, Guo, Wang and Qiang, gen. et sp. nov.

Etymology. From '*béret*', French, that designates a soft, visorless cap referring to the overall shape of this species, and 'spinosa', an adjective (Latin), alluding to its spiny ornament.

Holotype. CUBar138-12 (Fig. 1a–c).
Paratype. CUBar171-5 Fig. 1h, i) and CURBar121-8 (Fig. 1j, k).

Diagnosis. Body with a beret-like lateral profile. Convex side (presumably dorsal) with an elevated (presumably posterior) and lower (presumably anterior one) end. The opposite side (presumably ventral) flattened. Bilateral symmetry well expressed in the overall body shape (sagittal plane) and sclerite distribution. Antero-posterior polarity. Convex side with a slightly elevated sagittal stripe topped with a single row of four aligned spines (S1) and five additional spines (S2) on each side. Six broad-based conical sclerites (S3) distributed in two symmetrical longitudinal rows plus two sagittal ones. Double rows of six marginal spines (S4 and S5). Flattened side often pushed in and partly missing, bearing a possible mouth opening. Possible oral spine.

Stratigraphy and locality. *Watsonella crosbyi* Assemblage Zone(Guo et al., 2021), Member 5 of the Yanjiahe Formation (Cambrian Terreneuvian, Stage 2) in the Yanjiahe section near Yichang City, Hubei Province, China (Supplementary Figs. 1, 2).

Description and comparisons

The body of *Beretella spinosa* is secondarily phosphatized and has a consistent beret-like three-dimensional shape in the lateral view. Its maximum length, width, and height range from 1.0–2.9 mm, to 975–2450 µm, and 500–1000 µm, respectively (Fig. 1, Supplementary Tables 1–3). The ratio of the maximal length to width is 1.6:1 (Supplementary Fig. 3). As seen in top view, *B. spinosa* shows a small lateral constriction at approximately mid-length (Fig. 1a, c).

The body has a convex, assumedly dorsal side with one, presumably posterior

end more elevated than the other (Fig. 1b, e, i, k). This elevation is gradual along the sagittal plane and then becomes more abrupt near the low elevated, presumably anterior end. The opposite, assumedly ventral side is less well preserved and seems to have been originally flattened.

The convex side bears a complex ornamented pattern made of five sets (S1–S5) of spiny sclerites directed towards the more elevated end (Figs. 1a, b, d, e, h–k, 2a, b, d). These sclerites were originally pointed (Figs. 1a, d, e, 2b, k, l, Supplementary Fig. 4a, b, g), but most of them were broken thus revealing an internal cavity and an ellipsoidal transverse section (Figs. 1a, b, h–k, 2a–e, g). The broken sclerites show an inner and outer phosphatic layer (thickness ca. 20 to 50 µm) often separated by a thin empty space (Fig. 2g–l).

The convex side bears six prominent conical sclerites (S3) all with a rounded to elliptical well-delimited broad base, distributed in two longitudinal symmetrical pairs with two additional sclerites at both ends of the sagittal plane (Figs. 1, 2d, Supplementary Figs. 3e–h, 4e–i). A low-relief stripe runs in a sagittal position and vanishes towards the elevated end. It is topped by a row of aligned spines (S1, Fig. 1a); the one closer to the more elevated end being more tubular and longer. This row is flanked on both sides by smaller aligned spines (S2, Figs. 1a, d, h, 2a–c). Two relatively sinuous rows of six tiny spines are present parallel to the lateral margins (S4 and S5, Figs. 1b, e, h–j, 2d, e).

The convex side bears a polygonal micro-ornament (mesh size ca. 5 µm wide, Fig. 2f, Supplementary Tables 1–3). However, its exact extension is uncertain due to coarse secondary phosphatization. Clusters of spherical phosphatized grains (diameter ca. 20 µm) occur near the sclerite base (Supplementary Fig. 4b).

In most specimens, the flattened side is occupied by a relatively large opening (1200 and 600µm in maximal length and width, respectively) with irregularly defined margins (Fig. 1c, f, see also supplementary information movies 1, 2). The flattened side is often largely missing and opens into a spacious internal cavity with no signs of internal organs (e.g. gut and pharynx) (Fig. 1c, f). One specimen shows a tiny spine on the margin of the flattened side (Fig. 1f, g), which differs from other spiny sclerites (S1-S5).

The length of studied specimens ranges from 1.0 to 2.9 mm (Supplementary Fig. 3e–h). Whether growth was continuous or instead took place via successive moulting stages and cuticular renewal (ecdysis) could not be tested due to the small number of specimens (N=17) available for measurements. No major morphological variations (e.g. a sclerite pattern) can be seen between the smallest and largest specimens of B. spinosa (Supplementary Fig. 3e–h).

Remarks

Body polarities in *Beretella*

The anterior-posterior (AP) and dorsal-ventral (DV) polarities of *Beretella* are uneasy to define because of the lack of modern equivalent among extant

animals. In the vast majority of extinct and extant invertebrates for which antero-posterior polarity is defined on the basis of independent criteria (e.g. position of mouth), sclerites point backwards (e.g. Cambrian scalidophoran worms (Han et al., 2007; Huang et al., 2004) and *Wiwaxia* (Zhang et al., 2015b)). This is most probably also the case with *Beretella* (Fig. 1a, d, j). The dorsoventral polarity of *Beretella* is supported by the fact that protective sclerites such as spines most commonly occur on the dorsal side of bilaterians (Fig. 1a, d, j).

Comparison with *Saccorhytus* and other ecdysozoans

Beretella spinosa has no exact equivalent in any Cambrian animals except *Saccorhytus coronarius*, an enigmatic, sac-like ecdysozoan(Han et al., 2017; Liu et al., 2022; Shu and Han, 2020b). Both forms share a tiny, poorly differentiated ellipsoidal body, and a set of prominent bilaterally arranged spiny sclerites. Indeed, the broad-based conical sclerites (S3) of *Beretella* are almost identical to those of *Saccorhytus* (Supplementary Fig. 4c) and have counterparts among scalidophoran worms (Supplementary Fig. 4d). However, they differ in number, ornamented structures, shape, and spatial arrangement (see details in Supplementary Tables 1–3) which makes the hypothesis of *Saccorhytus* being the larval stage of *Beretella* unlikely. Both *Beretella* and *Saccorhytus* differ from other known ecdysozoans in the lack of a vermiform body, introvert, annulations, and through gut (Supplementary Tables 1–3).

Discussion

Ventral mouth. All bilaterian animals have a digestive system with at least one opening that corresponds to the mouth(Brusca et al., 2016). Although the presumed oral area of *Beretella* is poorly preserved (ventral side often pushed in and largely destroyed), its mouth is likely to be found ventrally (see description), since no other opening occurs on its dorsal side, except those created by broken sclerites. The well-defined dorsoventral polarity of *Beretella* would suggest that the animal was resting on its ventral (flattened) side, the spiny dorsal side playing a protective role. Maintaining ventral contact with a substrate seems to be very unlikely unless these microscopic ellipsoidal animals were interstitial.

Phylogenetic position of *Beretella*. *Beretella*'s phylogenetic affinities remain elusive due to the lack of information concerning its internal anatomy and ventral side. Its scleritome consists of isolated conical sclerites that were the cuticular outgrowths of a seemingly rigid integument that covered both sides of the animal. Such conical sclerites have close counterparts in Cambrian ecdysozoans such as scalidophoran worms (e. g. *Eokinorhynchus*(Zhang et al., 2015a)), lobopodians (e.g. *Onychodictyon ferox*(Hou et al., 1991)) and even more clearly *Saccorhytus* that recent cladistic analyses resolved as a branch of the total-group Ecdysozoa (Liu et al., 2022). These sclerites unknown in

other animal groups, suggest that both *Saccorhytus* and *Beretella* belongs to Ecdysozoa in the absence of more direct fossil evidence such as exuviae or features suggesting cuticular moulting(Daley and Drage, 2016; Wang et al., 2019).

Cladistic analyses were performed to test the relation of *Beretella* and *Saccorhytus* to other ecdysozoan groups and, more generally, their phylogenetic relationships with other bilaterian groups (see details in Supplementary Table 4). Both taxa join in a clade (Saccorhytida, Fig. 3a–c) that is resolved as stem species within total-group Ecdysozoa and as the sister group of Cycloneuralia plus Panarthropoda, i.e. crown-group Ecdysozoa (Figs. 3d, 4, Supplementary Figs. 6-9). These results are consistent with the body plan of Saccorhytida being markedly different from that of crown-group ecdysozoans that all have a vermiform body and differentiated structures such as the introvert and pharyngeal complex (Fig. 4).

The ancestral ecdysozoan body plan

Molecular clock analyses often place the divergence of Ecdysozoa relatively deep into the Ediacaran (Howard et al., 2022; Rota-Stabelli et al., 2013), thus highlighting major discrepancy with the known fossil record of the group. Potential ecdysozoans occur in the late Precambrian as suggested by 1) sclerites resembling those of extant priapulids, found in Ediacaran Small Carbonaceous Fossils assemblages(Moczydłowska et al., 2015) and 2) locomotion traces presumably made by scalidophoran worms (Buatois et al., 2014; Vannier et al., 2010). In the absence of fossil data for other vermiform groups such as nematoids, scalidophorans are potentially the oldest known representatives of Ecdysozoa. Recent Bayesian analyses based on a large molecular data set obtained from the 8 extant ecdysozoan phyla recover Scalidophora as the sister-group to Nematoida + Panarthropoda and suggest that ecdysozoans probably diverged in the Ediacaran possibly some 23 million years before the oldest fossil occurrence (trace fossils) of the group (Howard et al., 2022). Although this study does not speculate on the nature of the last common ancestor of Ecdysozoa, it is consistent with the view that the earliest representatives of the group were probably vermiform. Howard et al. (Howard et al., 2022) drew comparable conclusions based on *Acosmia*, an assumed stem-ecdysozoan worm from early Cambrian Chengjiang Lagerstätte. However, the re-evaluation of the morphological characteristics of this worm rather suggests a less basal position either within the total-group Cycloneuralia (Fig. 3d, Supplementary Figs. 6, 7) or among crown-group Ecdysozoa (Supplementary Figs. 8, 9). The non-vermiform nature of saccorhytids and their position as the sister group of the crown-group Ecdysozoa clearly reopens the debate on the nature of the ancestral ecdysozoan (Fig. 4) and suggests exploring various evolutionary hypotheses, in particular: 1) does the enigmatic saccorhytid body plan results from anatomical simplification? 2) to what extent may these animals shed light on the nature of the earliest

ecdysozoans?

Do saccorhytids result from simplification?

A relatively simple body plan and tiny size is often seen as resulting from anatomical simplification (e.g. digestive system) and miniaturization (micrometric size) in possible relation with the adaptation to specialized ecological niches or parasitism (Hanken and Wake, 1993). For example, some extant scalidophoran worms living in interstitial (meiobenthic) habitats such as loriciferans have a miniaturized body (Kirstensen, 1983) compared with their macroscopic counterparts (e.g. *Priapulus*(Schmidt-Rhaesa, 2013b)). However, they retain a through gut and a functional introvert and show no sign of drastic internal simplification (Schmidt-Rhaesa, 2013a). Anatomical reduction is a typical feature of parasitism(Hanken and Wake, 1993) that is well-represented among extant ecdysozoans such as nematodes(Schmidt-Rhaesa, 2014). Although relatively small (ca. 0.1-2.5 mm long), nematodes underwent no simplification of their digestive system. Saccorhytids have no specialized features (e.g. anchoring or piercing structures) that would point to any adaptation to ecto- or endo-parasitic lifestyles(Cong et al., 2017). *Saccorhytus* has been interpreted[16] as a possible interstitial animal based on its micrometric size which corresponds to that the of the extant meiofauna. If we accept the hypothesis of saccorhytids resulting from simplification, then we need to determine its origin. Simplification of saccorhytids from a vermiform animal (e.g. cycloneuralian worm with a through gut and terminal mouth) is difficult to conceive because it would involve considerable anatomical transformations such as the loss of vermiform organization, introvert and pharynx in addition to that of the digestive system (Fig. 4). Alternative options to consider are ancestral and not necessarily vermiform ecdysozoans.

Early evolution of ecdysozoans: a new scenario

We propose here an alternative evolutionary hypothesis (Fig. 4) in which saccorhytids are replaced within the broader framework of the origin and early diversification of moulting animals. Saccorhytids are seen as an early off-shot from the stem-line Ecdysozoa (see cladistic analysis above) that possibly retained important features of the body plan of ancestral non-vermiform ecdysozoans (see ancestral character state reconstruction in Supplementary Table 4). This scenario must be considered as a working hypothesis whose aim is to stimulate research in this key area of animal evolution.

The cuticular secretion and the loss of cilia (Valentine and Collins, 2000) are seen as the first of a series of evolutionary events (Fig. 4) that led to the rise of Ecdysozoa. Moulting (shedding of the old cuticle via apolysis and its renewal) further reconciled body growth and cuticular protection (Schmidt-Rhaesa, 2007). Cuticle secretion and moulting may have been quasi-simultaneous innovations that took place over a relatively short time interval. The nature of the very first ecdysozoans is hypothetical and lacks fossil evidence. However,

they are tentatively represented here as small epibenthic or interstitial slow-moving non-vermiform animals from which saccorhytids may have evolved via an assumed anatomical simplification (i.e. loss of anus seen details in Supplementary Table 4, Fig. 4).

In our scenario, this ancestral ecdysozoan stock would have also given rise to vermiform ecdysozoans through stepwise anatomical transformations such as the body elongation, the differentiation of key morpho-functional structures such as the pharynx and the introvert and the shift of the ventral mouth to a terminal position (Martín-Durán and Hejnol, 2015) (Fig. 4). This mouth shift from ventral to terminal arising in crown ecdysozoans is consistent with the chronology of divergence of animal lineages and the fact that the mouth of most spiralians is ventral (Martín-Durán and Hejnol, 2015; Nielsen, 2019; Ortega-Hernandez et al., 2019). Developmental studies show that embryos of extant cycloneuralians have a ventral mouth that moves to a terminal position towards the adult stage (Martín-Durán and Hejnol, 2015; Nielsen, 2019). These assumed major anatomical changes (e.g. functional introvert) must be placed in the ecological context of Cambrian animal radiation. Important changes in the functioning of marine ecosystems occurred in the early Cambrian such as interactive relationships between animal species, exemplified by predation (Vannier and Chen, 2005; Vermeij, 1977) may have acted as drivers in the evolution of early ecdysozoans, in promoting burrowing into sediment and the colonization of endobenthic habitats for the first time (Vannier et al., 2010). Burrowing into the sediment could be seen as the evolutionary response of epibenthic animals such as ancestral ecdysozoans to escape visual predation(Daley et al., 2013; Vannier and Chen, 2005). This migration to endobenthic shelters was made possible by the development of a resistant cuticular layer (Fig. 4) that strongly reduced physical damage caused by friction with the sediment and provided anchoring points (e.g. scalids and sclerites). Whereas saccorhytids became rapidly extinct during the Cambrian, worms massively colonized endobenthic habitats, resulting in bioturbation and ecological turnover.

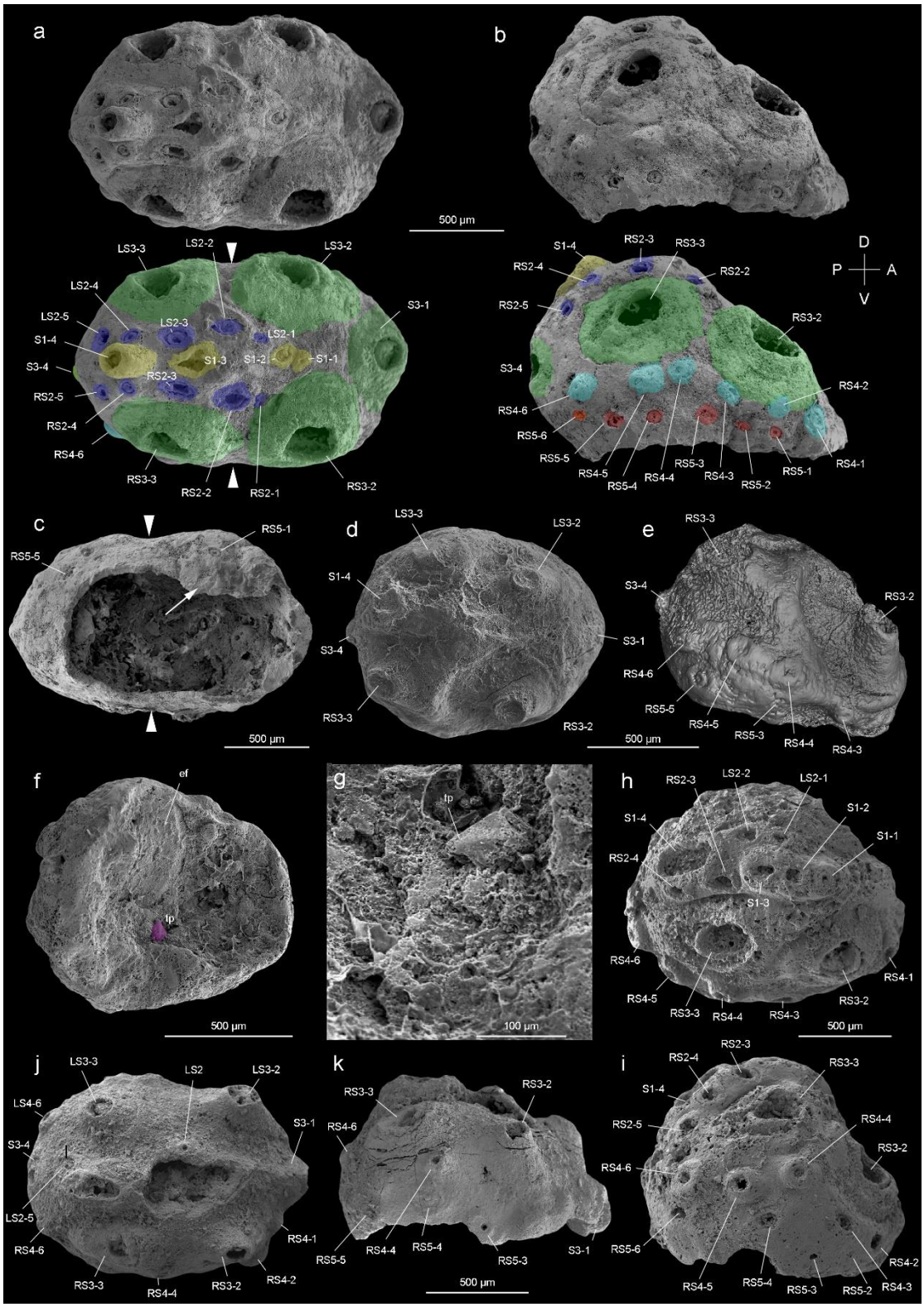

Fig. 1. *Beretella spinosa* gen. et sp. nov. from Member 5 of the Yanjiahe Formation (Cambrian Stage 2), Yichang, Hubei Province, China. a–c, Holotype, CUBar138-12. **a**, Dorsal view showing the external ornament: (five sclerites at the midline in yellow (S1); flanked by two rows of sclerites in blue (S2); large broad-based conical sclerites in two dorsolateral pairs and one antero-posterior pairs in green (S3)); white arrows indicate lateral constriction.

b, Right lateral view showing two additional rows of six sclerites (S4 and S5, in light blue and pink, respectively). **c**, Ventral view showing a large opening that may have accommodated the mouth (see the text) and an empty body cavity. **d–g**, CUBar75-45. **d**, Dorsal view showing a broken S3. **e**, Micro-CT image, right lateral view displaying S4. **f**, Ventral view depicting a tiny projection in purple. **g**, An enlargement of the projection of **f**. **h–i**, Paratype, CUBar171-5. **h**, Right dorsal view showing S1–S4. **i**, Right-lateral view showing S4 and S5. **j–k**, Paratype CUBar121-8. **j**, Dorsal view showing poorly preserved S1 and S2. **k**, Right-lateral view showing S3–S5. A, assumed anterior end (see text); ef, exotic fragment; D, assumed dorsal side; L, left; P, posterior end; R, right; tp, tiny spine; V, ventral side. The same abbreviations are used throughout the manuscript including Supplementary materials.

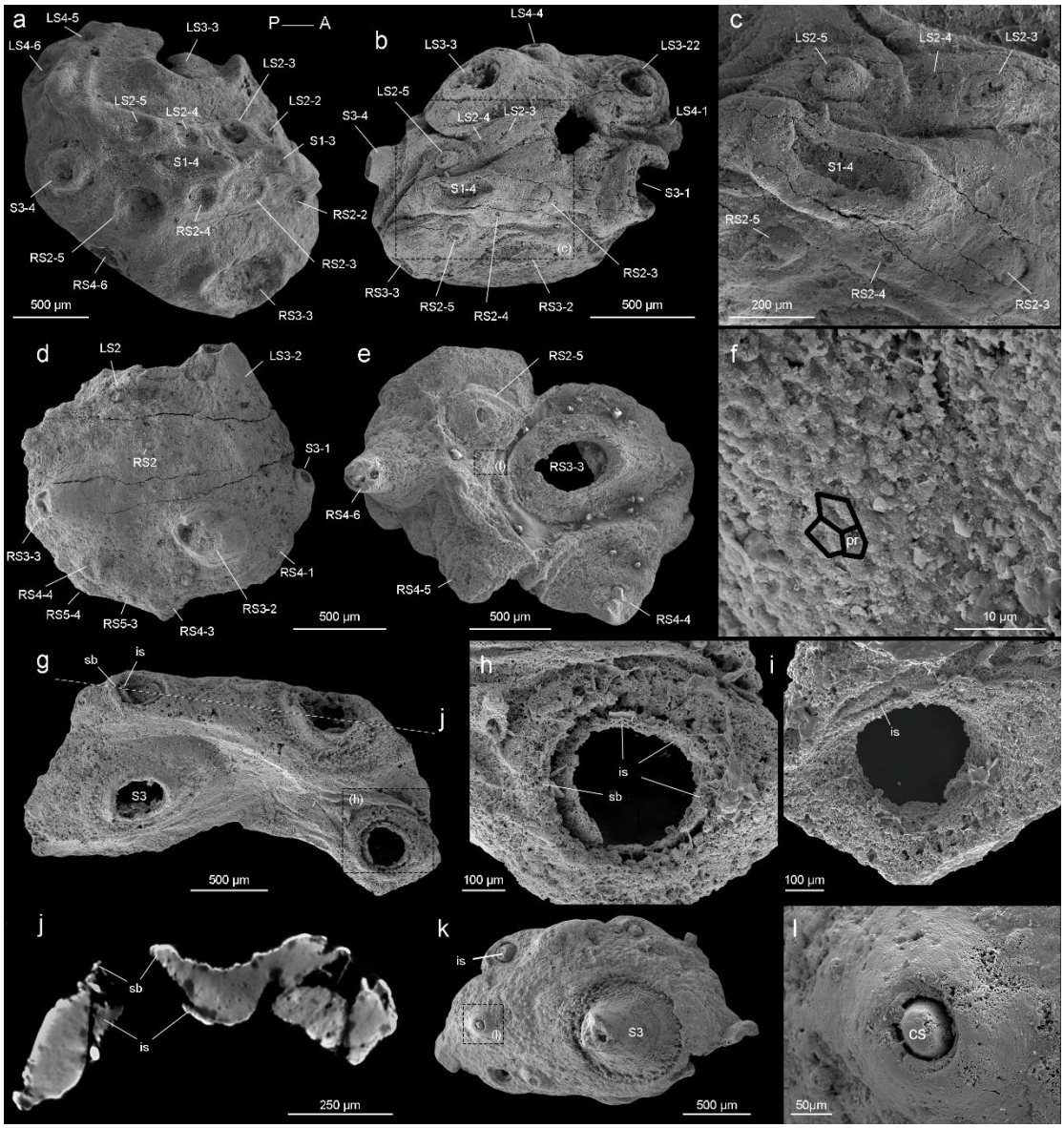

Fig. 2. *Beretella spinosa* gen. et sp. nov. a, CUBar99-19, dorsal view showing an ornament S1–S4. **b–c**, CUBar136-9, general dorsal view and

details. **d**, CUBar136-11, dorsal view showing S1–S5. **e–f**, CUBar73-15 general view and details of the cuticular polygonal reticulation in black. **g–j**, CUBar128-27. **g–i**, general view and details of the bi-layered structure of the cuticular wall as seen in broken conical sclerites. **j**, Micro-CT section showing possibly sclerite infilling. **k-l**, CUBar99-18, cuticular fragment, general view and details of large sclerite (central feature represents possible phosphatic infilling). is, infilling sclerite; pr, polygonal reticulation; sb, sclerite base.

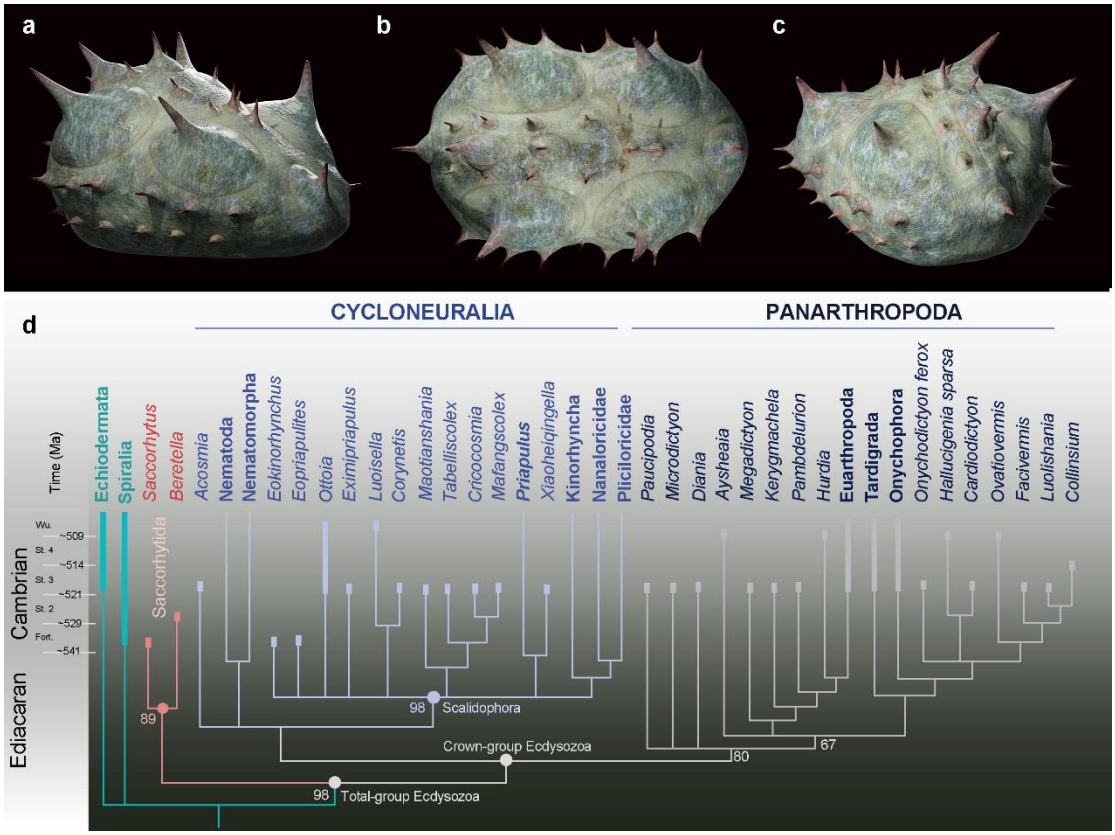

Fig. 3. Position of *Beretella spinosa* in the animal tree based on cladistic analysis. a-c, artistic three-dimensional reconstructions of *Beretella spinosa* in the anterolateral, dorsal, and posterolateral views. **d**, Animal tree obtained from cladistic analyses using maximum likelihood tree obtained from cladistic analyses using maximal likelihood (IQTREE). *Saccorhytus* and *Beretella* join in a clade (new phylum Saccorhytida) resolved as the sister-group of all other ecdysozoans; numbers at key nodes denote probability. Fossil and extant taxa are in italics and bold, respectively. Known fossil record indicated by thicker bars (after (Shu and Han, 2020a)).

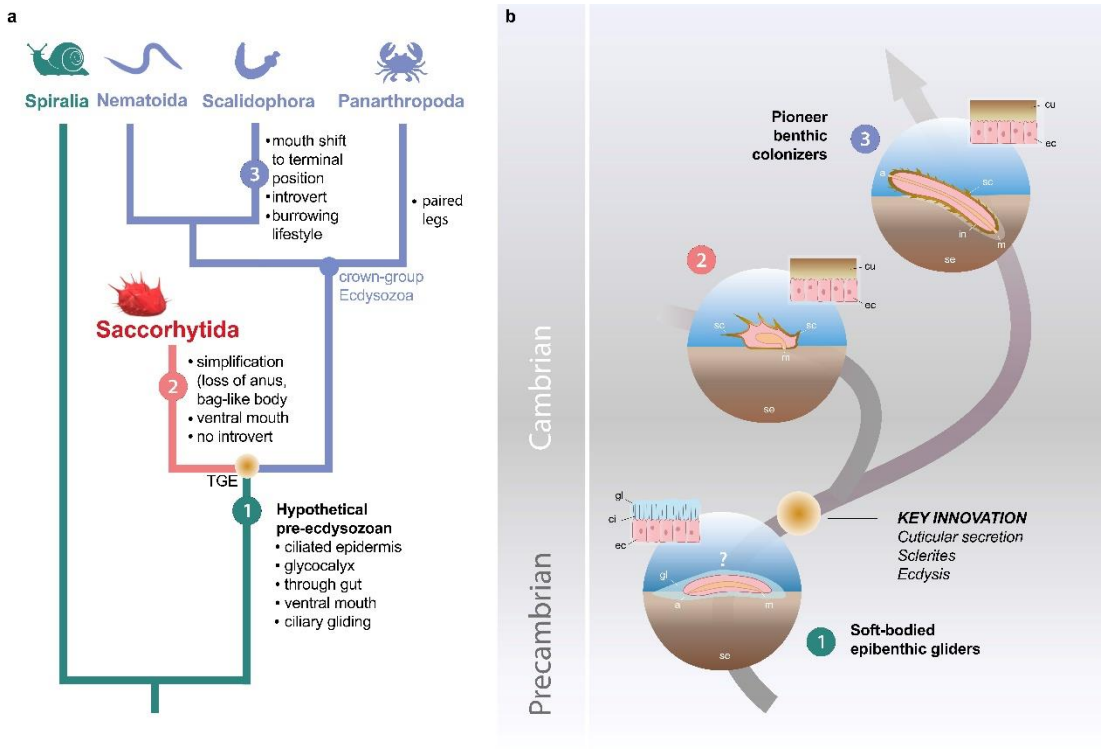

Fig. 4. Possible evolutionary scenario to explain the origin and early evolution of ecdysozoans. **a**, Summary tree (see Supplementary Figs. 6-9) showing saccorhytids as a sister-group of Cycloneuralia (Nematoida plus Scalidophora) + Panarthropoda; main morphological features of each group listed along each branch. **b**, Potential evolutionary pathway to evolve Saccorhytida and crown-group Ecdysozoa. Numbers in green, red and blue circles designate pre-ecdysozoan (Spiralia), Saccorhytida and Cycloneuralia, respectively. Light brown gradient (circle) to emphasize ecdysis and sclerite secretion seen as key evolutionary steps. 1, Hypothetical pre-ecdysozoan animal with a ciliated epidermis and glycocalyx. 2, Saccorhytid exemplified by *Beretella* with a cuticle bearing sclerites and a simplified internal organization (e.g. loss of anus). 3, Crown-group ecdysozoan exemplified by a scalidophoran worm with an elongated shape, a differentiated head (introvert) and trunk, sclerites, a through gut, a terminal mouth and abilities to burrow into bottom sediment. Animals not to scale. Abbreviations: a, anus; ci, cilia; cu, cuticle; ec, epidermal cell; gl, glycocalyx (mucous layer); m, mouth; in, introvert; sc, sclerite; se, sediment; TGE, total-group Ecdysozoa. Silhouettes from phylopic.org.

Methods

Material

Fourteen specimens of *Beretella spinosa* were recovered from samples (siliceous-phosphatic, intraclastic limestone) collected from Member 5 of the Yanjiahe Formation, Yanjiahe section near Yichang City, Hubei Province, China(Guo et al., 2021) (Supplementary Tables 1–3). These were obtained by digesting the rocks in 10% acetic acid. Faunal elements associated with *Beretella spinosa* (Supplementary Tables 1–3) in residues are mainly tiny molluscs (CUBar21-4 and CUBar206-6). Comparisons were made with 10 specimens of *Saccorhytus coronarius* (ELIXX25-62, ELIXX34-298, ELIXX45-20, ELIXX48-64, ELIXX58-336, ELIXX61-27, ELIXX65-116, ELIXX65-296, ELIXX99-420) and one coeval scalidophoran specimen (ELIXX57-320) all from Bed 2 of the Kuanchuanpu Formation, Zhangjiagou section near Xixiang County, south Shaanxi Province, China. All specimens of *Beretella* are deposited in the paleontological collections of Chang'an University, Xi'an (CU), those of scalidophoran, and *Saccorhytus* at Northwest University, Xi'an (ELI), China.

Scanning electron microscopy (SEM)

All specimens were coated with gold and then imaged using a FEI Quanta 400 FEG SEM at Northwest University and a FEI Quanta 650 at Chang'an University.

X-ray computed microtomography and 3D reconstruction

Micro-CT-images (tiff format, with pixel size 1.1 µm) of *Beretella* (CUBar75-45, CUBar128-27, CUBar138-12) and *Saccorhytus* (ELIXX65-116, ELIXX99-420) were acquired using the Zeiss Xradia 520 at Northwest University (NWU), Xi'an, China, at an accelerating voltage of 50 kV and a beam current of 80 µA. Micro-CT data were processed using VGstudio Max 3.2 for 3D volume rendering.

Measurements

Measurements of the length, width, and height of *Beretella* and *Saccorhytus* were obtained from Micro-CT and SEM images by using tipDig2 v.2.16.

Phylogenetic analysis

We built our matrix with 55 taxa coded using 191 morphological characteristics (Supplementary Texts 1, 2). It is largely based on the data published by Howard et al.(Howard et al., 2020), Vinther and Parry(Vinther and Parry, 2019) and Ou et al.(Ou et al., 2017), although emended and supplemented by recent updates and new observations (Supplementary Text 1). Three characters (37. Through gut, 38. U-shaped gut, and 40. Ventral mouth) in matrix were coded as "? (uncertain)", "?", and "?", respectively. Because although we can infer a

ventral mouth and no anus of *Beretella*, these anatomic structures are invisible in fossils. We analyzed the data matrix using parsimony (TNT), likelihood (IQTREE) and Bayesian inference (MrBayes). Parsimony analysis was implemented in TNT under equal and implied (k=3) weight. Parameters are default (Goloboff et al., 2008; Goloboff and Catalano, 2016). The maximum-likelihood tree search was conducted in IQ-TREE(Nguyen et al., 2015), and support was assessed using the ultrafast phylogenetic bootstrap replication method (Hoang et al., 2018; Minh et al., 2013) to run 50,000 replicates. Bayesian inference was conducted in with MrBayes v3.2.6a with default priors and Markov chain Monte Carlo settings(Ronquist et al., 2012). Two independent runs of 7,000,000 Markov chain Monte Carlo generations were performed, each containing four Markov chains under the Mkv + Γ model for the discrete morphological character data(Lewis, 2001). In each run (N=2), trees were collected at a sampling frequency of every 5,000 generations and with the first 25% samples discarded as burn-in. The convergence of chains was checked by effective sample size (ESS) values over 1,000 in Tracer v.1.7(Rambaut et al., 2018), 1.0 for the potential scale reduction factor (PSRF)(Gelman and Rubin, 1992), and by an average standard deviation of split frequencies below 0.007.

Ancestral character state reconstructions

Ancestral character state reconstructions for six morphological characters were performed on the ecdysozoan total group node, the ecdysozoan crown group node and saccorhytid node. Characters selected for ancestral state reconstruction represent traits inferred as ecdysozoan plesiomorphies (ancestral characters) from studies of crown group taxa. These characters included the presence or absence of: (1) through gut; (2) ventral mouth; (3) introvert (see Supplementary Table 4).

This was carried out individually for the selected character in MrBayes. This was employed to calculate the posterior probability of the presence (1) and absence (0) of the selected characters at the selected nodes. Analyses used the MK + gamma model, and always converged after 2 million generations. Average deviation of split frequencies (< 0.01), ESS scores (> 200), and PSRF values (= approx. 1.00) assessed convergence of the MCMC chains (Howard et al., 2020).

Data availability

The data that support the findings of this study are available in the recent paper and its Supplementary Information.

References and Notes

Aguinaldo, A.M.A., Turbeville, J.M., Linford, L.S., Rivera, M.C., Garey, J.R., Raff, R.A. and Lake, J.A., 1997. Evidence for a clade of nematodes,

arthropods and other moulting animals. Nature, 387(6632): 489-93.

Brusca, R.C., Moore, W. and Shuster, S.M., 2016. Invertebrates. Sinauer Associates, Inc., Sunderland Massachusetts USA, 639-910 pp.

Buatois, L.A., Narbonne, G.M., Mangano, M.G., Carmona, N.B. and Myrow, P., 2014. Ediacaran matground ecology persisted into the earliest Cambrian. Nat Commun, 5: 3544.

Budd, G.E., 2001. Why are arthropods segmented? Evolution & Development, 3(5): 332–342.

Cong, P., Ma, X., Williams, M., Siveter, D.J., Siveter, D.J., Gabbott, S.E., Zhai, D., Goral, T., Edgecombe, G.D. and Hou, X., 2017. Host-specific infestation in early Cambrian worms. Nature Ecology & Evolotion, 1(10): 1465-1469.

Daley, A.C. and Drage, H.B., 2016. The fossil record of ecdysis, and trends in the moulting behaviour of trilobites. Arthropod Structure & Development, 45(2): 71-96.

Daley, A.C., Paterson, J.R., Edgecombe, G.D., García-Bellido, D.C., Jago, J.B. and Donoghue, P., 2013. New anatomical information on *Anomalocaris* from the Cambrian Emu Bay Shale of South Australia and a reassessment of its inferred predatory habits. Palaeontology, 56: 971-990.

Erwin, D.H., 2020. The origin of animal body plans: a view from fossil evidence and the regulatory genome. Development, 147(4): dev182899.

Gelman, A. and Rubin, D.B., 1992. Inference from iterative simulation using multiple sequences (with discussion). Statistical Science, 7: 457-472.

Goloboff, P.A., Carpenter, J.M., Arias, J.S. and Esquivel, D.R.M., 2008. Weighting against homoplasy improves phylogenetic analysis of morphological data sets. Cladistics, 24(5): 758-773.

Goloboff, P.A. and Catalano, S.A., 2016. TNT version 1.5, including a full implementation of phylogenetic morphometrics. Cladistics, 32: 221-238.

Guo, J.-F., Li, G.-X., Qiang, Y.-Q., Song, Z.-C., Zhang, Z.-F., Han, J. and Wang, W.-Z., 2021. *Watsonella crosbyi* from the lower Cambrian (Terreneuvian, Stage 2) Yanjiahe Formation in Three Gorges Area, South China. Palaeoworld, 30(1): 1-19.

Han, J., Conway Morris, S., Ou, Q., Shu, D.G. and Huang, H., 2017. Meiofaunal deuterostomes from the basal Cambrian of Shaanxi (China). Nature, 542(7640): 228-231.

Han, J., Liu, J.N., Zhang, Z.F., Zhang, X.L. and Shu, D.G., 2007. Trunk ornament on the palaeoscolecid worms *Cricocosmia* and *Tabelliscolex* from the Early Cambrian Chengjiang deposits of China. Acta Palaeontologica Polonica, 52(2): 423–431.

Hanken, J. and Wake, D.B., 1993. Miniaturization of body size: Organismal consequences and evolutionary significance. Annual Review of Ecology and Systematics, 24: 501-519.

Hoang, D.T., Chernomor, O., von Haeseler, A., Minh, B.Q. and Vinh, L.S., 2018.

UFBoot2: Improving the Ultrafast Bootstrap Approximation. Mol Biol Evol, 35(2): 518-522.

Hou, X.G., Ramskold, L. and Bergstrom, J., 1991. Composition and preservation of the Chengjiang fauna -a Lower Cambrian soft-bodied biota. Zoologica Scripta, 20(4): 395-411.

Howard, R.J., Edgecombe, G.D., Shi, X., Hou, X. and Ma, X., 2020. Ancestral morphology of Ecdysozoa constrained by an early Cambrian stem group ecdysozoan. BMC Evolutionary Biology, 20(1): 156.

Howard, R.J., Giacomelli, M., Lozano-Fernandez, J., Edgecombe, G.D., Fleming, J.F., Kristensen, R.M., Ma, X., Olesen, J., Sørensen, M.V., Thomsen, P.F., Wills, M.A., Donoghue, P.C.J. and Pisani, D., 2022. The Ediacaran origin of Ecdysozoa: integrating fossil and phylogenomic data. Journal of the Geological Society, 179: jgs2021-107.

Huang, D., Vannier, J. and Chen, J., 2004. Anatomy and lifestyles of Early Cambrian priapulid worms exemplified by Corynetis and Anningvermis from the Maotianshan Shale (SW China). Lethaia, 37(1): 21-33.

Kirstensen, R.M., 1983. Loricifera, a new phylum with Aschelminthes characters from the meiobenthos. Zeitschrift für zoologische Systematik und Evolutionsforschung, 21(3): 163-180.

Laumer, C.E., Fernandez, R., Lemer, S., Combosch, D., Kocot, K.M., Riesgo, A., Andrade, S.C.S., Sterrer, W., Sorensen, M.V. and Giribet, G., 2019. Revisiting metazoan phylogeny with genomic sampling of all phyla. Proceedings of the Royal Society B, 286(1906): 20190831.

Lewis, P.O., 2001. A likelihood approach to estimating phylogeny from discrete morphological character data. Systematic biology, 50(6): 913-925.

Liu, A.G., Matthews, J.J., Menon, L.R., McIlroy, D. and Brasier, M.D., 2014. Haootia quadriformis n. gen., n. sp., interpreted as a muscular cnidarian impression from the Late Ediacaran period (approx. 560 Ma). Proc Biol Sci, 281(1793).

Liu, Y., Carlisle, E., Zhang, H., Yang, B., Steiner, M., Shao, T., Duan, B., Marone, F., Xiao, S. and Donoghue, P.C.J., 2022. *Saccorhytus* is an early ecdysozoan and not the earliest deuterostome. Nature, 609: 541-546.

Martín-Durán, J.M. and Hejnol, A., 2015. The study of *Priapulus caudatus* reveals conserved molecular patterning underlying different gut morphogenesis in the Ecdysozoa. BMC Biology, 13: 29.

Minh, B.Q., Nguyen, M.A. and von Haeseler, A., 2013. Ultrafast approximation for phylogenetic bootstrap. Mol Biol Evol, 30(5): 1188-95.

Moczydłowska, M., Budd, G.E. and AgiĆ, H., 2015. Ecdysozoan-like sclerites among Ediacaran microfossils. Geological Magazine, 152(06): 1145-1148.

Nguyen, L.T., Schmidt, H.A., Von Haeseler, A. and Minh, B.Q., 2015. IQ-TREE: a fast and effective stochastic algorithm for estimating maximum-likelihood phylogenies. Molecular biology and evolution,

584 32(1): 268-274.
585 Nielsen, C., 2019. Was the ancestral panarthropod mouth ventral or terminal?
586 Arthropod Structure & Development, 49: 152-154.
587 Ortega-Hernandez, J., Janssen, R. and Budd, G.E., 2019. The last common
588 ancestor of Ecdysozoa had an adult terminal mouth. Arthropod
589 Structure & Development, 49: 155-158.
590 Ou, Q., Han, J., Zhang, Z., Shu, D., Sun, G. and Mayer, G., 2017. Three
591 Cambrian fossils assembled into an extinct body plan of cnidarian
592 affinity. Proceedings of the National Academy of Science, 114(33):
593 8835-8840.
594 Rambaut, A., Drummond, A., Xie, D., Baele, G. and Suchard, M., 2018.
595 Posterior summarisation in Bayesian phylogenetics using Tracer 1.7.
596 Systematic Biology, 67(5): 901-904.
597 Ronquist, F., Teslenko, M., van der Mark, P., Ayres, D.L., Darling, A., Hohna, S.,
598 Larget, B., Liu, L., Suchard, M.A. and Huelsenbeck, J.P., 2012.
599 MrBayes 3.2: efficient Bayesian phylogenetic inference and model
600 choice across a large model space. Systematic Biology, 61(3): 539-42.
601 Rota-Stabelli, O., Daley, A.C. and Pisani, D., 2013. Molecular timetrees reveal
602 a Cambrian colonization of land and a new scenario for ecdysozoan
603 evolution. Current Biology, 23(5): 392-8.
604 Sawaki, Y., Nishizawa, M., Suo, T., Komiya, T., Hirata, T., Takahata, N., Sano,
605 Y., Han, J., Kon, Y. and Maruyama, S., 2008. Internal structures and U–
606 Pb ages of zircons from a tuff layer in the Meishucunian formation,
607 Yunnan Province, South China. Gondwana Research, 14(1-2):
608 148-158.
609 Schmidt-Rhaesa, A., 2007. The evolution of organ systems. Oxford university
610 press, 54-73 pp.
611 Schmidt-Rhaesa, A., 2013a. Nematomorpha. In: A. Schmidt-Rhaesa (Editor),
612 Gastrotricha, Cycloneuralia and Gnathifera. De Gruyter, Germany, pp.
613 29-146.
614 Schmidt-Rhaesa, A., 2013b. Priapulida. In: A. Schmidt-Rhaesa (Editor),
615 Gastrotricha, Cycloneuralia and Gnathifera. De Gruyter, Germany, pp.
616 147-180.
617 Schmidt-Rhaesa, A., 2014. Handbook of Zoology. Gastrotricha, Cycloneuralia
618 and Gnathifera, 2. De Gruyter, Germany, 5-12 pp.
619 Shu, D.G. and Han, J., 2020a. The core value of Chengjiang fauna: the
620 formation of the animal kingdom and the birth of basic human organs.
621 Earth Science Frontiers, 27: 382-412.
622 Shu, D.G. and Han, J., 2020b. The core value of Chengjiang fauna: the
623 information of animal kingdom and the birth basic human organs. Earth
624 Science Frontiers, 27: 1-32.
625 Valentine, J.W. and Collins, A.G., 2000. The significance of moulting in
626 ecdysozoan evolution. Evolution & Development, 2(3): 152–156.
627 Vannier, J., Calandra, I., Gaillard, C. and Żylińska, A., 2010. Priapulid worms:

628 Pioneer horizontal burrowers at the Precambrian-Cambrian boundary.
629 Geology, 38(8): 711-714.
630 Vannier, J. and Chen, J., 2005. Early Cambrian Food Chain: New Evidence
631 from Fossil Aggregates in the Maotianshan Shale Biota, SW China.
632 Palaios, 20(1): 3-26.
633 Vermeij, G.J., 1977. The Mesozoic marine revolution: evidence from snails,
634 predators and grazer. Paleobiology, 3: 245-258.
635 Vinther, J. and Parry, L.A., 2019. Bilateral jaw elements in *Amiskwia*
636 *sagittiformis* bridge the morphological gap between gnathiferans and
637 chaetognaths. Current Biology, 29(5): 881-888 e1.
638 Wang, D., Vannier, J., Schumann, I., Wang, X., Yang, X.G., Komiya, T., Uesugi,
639 K., Sun, J. and Han, J., 2019. Origin of ecdysis: fossil evidence from
640 535-million-year-old scalidophoran worms. Proceedings of the Royal
641 Society B, 286(1906): 20190791.
642 Zhang, H., Xiao, S., Liu, Y., Yuan, X., Wan, B., Muscente, A.D., Shao, T., Gong,
643 H. and Cao, G., 2015a. Armored kinorhynch-like scalidophoran animals
644 from the early Cambrian. Scientific Reports, 5: 16521.
645 Zhang, Z., Smith, M.R. and Shu, D., 2015b. New reconstruction of the Wiwaxia
646 scleritome, with data from Chengjiang juveniles. Sci Rep, 5: 14810.
647

648

649 **Acknowledgments**: We thank H. G. for technical assistance. Funding: We
650 thank the National Natural Science Foundation of China (grants 42172016,
651 41890844 to J.G., 41621003 to J.H., 42202009 to D.W.), the Strategic Priority
652 Research Program of the Chinese Academy of Sciences (grant XDB26000000
653 grant to J.H. and J.G.), the China Post-doctoral Science Foundation (grant
654 2022M722568 to D.W.), the Key Scientific and Technological Innovation Team
655 Project in Shaanxi Province (grant to J.G.), and the Région Auvergne Rhône
656 Alpes and Université Claude Bernard Lyon 1 (grant to J.V.) for financial
657 support.
658

659 **Author contributions**: J.H. and J.G. conceived the research. J.G., Y.Q., Z.S.,
660 J.P., and B. Z. collected the material from Yanjiahe Formation. Y.Q. and D.W.
661 prepared all the specimens, photographs, figures except Figure 4 (J.V.). J.S.
662 performed the analysis by Micro-CT and visualization with Micro-CT data. D.W.
663 and J.H. performed phylogenetic analyses. Y.Y. performed morphospace
664 analyses and Y.Z. and T.Z. performed computational fluid dynamic analyses in
665 initial draft (not used in this version). D.W., J.V., J.H., J.G., and Y.Q. wrote the
666 paper with input from all other authors. All authors approved the final
667 manuscript.
668

669 **Competing interests:** The authors declare no competing interests.
670

671 **Additional information**

672 **Supplementary information** The online version contains supplementary
673 material (tomographic data of *Beretella* and *Saccorhytus*, and movies of
674 3D-animation of the holotype of *Beretella*) available at
675 https://figshare.com/s/054f31fc22567a590d7f.

676

677 **Correspondence and requests for materials** should be addressed to J. G.
678 or J. H.

679

680